Geophysical Research Letters

RESEARCH LETTER
10.1029/2020GL087669

River Inflow Dominates Methane Emissions in an Arctic Coastal System

Cara C. Manning[1], Victoria L. Preston[2,3], Samantha F. Jones[4], Anna P. M. Michel[2], David P. Nicholson[5], Patrick J. Duke[4,6], Mohamed M. M. Ahmed[4], Kevin Manganini[2], Brent G. T. Else[4], and Philippe D. Tortell[1,7]

[1]Department of Earth, Ocean and Atmospheric Sciences, University of British Columbia, Vancouver, BC, Canada, [2]Applied Ocean Physics and Engineering Department, Woods Hole, MA, USA, [3]Department of Aeronautics and Astronautics, Massachusetts Institute of Technology, Cambridge, MA, USA, [4]Department of Geography, University of Calgary, Calgary, AB, Canada, [5]Marine Chemistry and Geochemistry Department, Woods Hole Oceanographic Institution, Woods Hole, MA, USA, [6]Now at School of Earth and Ocean Sciences, University of Victoria, Victoria, BC, Canada, [7]Department of Botany, University of British Columbia, Vancouver, BC, Canada

Key Points:
- Methane concentrations in an Arctic estuary show strong seasonality; river inflow at the start of the freshet drives elevated concentrations
- Observations with a novel robotic kayak demonstrate that methane and carbon dioxide in the estuary are rapidly ventilated following ice melt
- River discharge is estimated to account for >95% of annual methane emissions from the estuary

Supporting Information:
- Supporting Information

Correspondence to:
C. C. Manning, A. P. M. Michel, and D. P. Nicholson,
cmanning@alum.mit.edu;
amichel@whoi.edu;
dnicholson@whoi.edu

Citation:
Manning, C. C., Preston, V. L., Jones, S. F., Michel, A. P. M., Nicholson, D. P., Duke, P. J., et al. (2020). River inflow dominates methane emissions in an Arctic coastal system. *Geophysical Research Letters*, *47*, e2020GL087669. https://doi.org/10.1029/2020GL087669

Received 24 FEB 2020
Accepted 14 APR 2020
Accepted article online 23 APR 2020

Abstract We present a year-round time series of dissolved methane (CH_4), along with targeted observations during ice melt of CH_4 and carbon dioxide (CO_2) in a river and estuary adjacent to Cambridge Bay, Nunavut, Canada. During the freshet, CH_4 concentrations in the river and ice-covered estuary were up to 240,000% saturation and 19,000% saturation, respectively, but quickly dropped by >100-fold following ice melt. Observations with a robotic kayak revealed that river-derived CH_4 and CO_2 were transported to the estuary and rapidly ventilated to the atmosphere once ice cover retreated. We estimate that river discharge accounts for >95% of annual CH_4 sea-to-air emissions from the estuary. These results demonstrate the importance of resolving seasonal dynamics in order to estimate greenhouse gas emissions from polar systems.

Plain Language Summary The primary cause of recent global climate change is increasing concentrations of heat-trapping greenhouse gases in the atmosphere. Ongoing rapid Arctic climate change is affecting the annual cycle of sea ice formation and retreat; however, most published studies of greenhouse gases in Arctic waters have been conducted during ice-free, summertime conditions. In order to characterize seasonal variability in greenhouse gas distributions, we collected year-round measurements of the greenhouse gas methane (CH_4) in a coastal Arctic system near Cambridge Bay, Nunavut, Canada. We found that during the ice melt season, river water contains methane concentrations up to 2,000 times higher than the wintertime methane concentrations in the coastal ocean. We utilized a novel robotic kayak to conduct high-resolution mapping of greenhouse gas distributions during ice melt. From these data, we demonstrate that the river water containing elevated levels of methane and carbon dioxide (CO_2) flowed into the coastal ocean, and when ice cover melted, these greenhouse gases were rapidly emitted into the atmosphere. We estimate that in this system, more than 95% of all annual methane emissions from the estuary are driven by river inflow.

1. Introduction

Methane (CH_4) emissions from Arctic waters and sediments may accelerate in the future as part of positive feedback from ongoing climate change (Biastoch et al., 2011; James et al., 2016; Shakhova et al., 2010). Landscapes that were once permanently frozen are now seasonally thawing, and the ice-free season is lengthening in freshwater and marine systems (Magnuson, 2000; Stroeve et al., 2012; Zona et al., 2016). Thawing can result in the mobilization of labile organic matter and emissions of greenhouse gases such as carbon dioxide (CO_2), methane (CH_4), and nitrous oxide (N_2O; Karlsson et al., 2013; Kvenvolden et al., 1993; Lamarche-Gagnon et al., 2019; Voigt et al., 2017; Zona et al., 2016). Studies of terrestrial and freshwater Arctic systems have demonstrated strong temporal variability in greenhouse gas emissions in these environments (Denfeld et al., 2018; Karlsson et al., 2013; Lamarche-Gagnon et al., 2019; Phelps et al., 1998; Voigt et al., 2017; Zona et al., 2016), yet published measurements in Arctic marine and estuarine waters are strongly biased toward summertime, low-ice conditions (Fenwick et al., 2017; Shakhova et al., 2010), establishing a need for long-term studies that characterize the full range of seasonal variability.

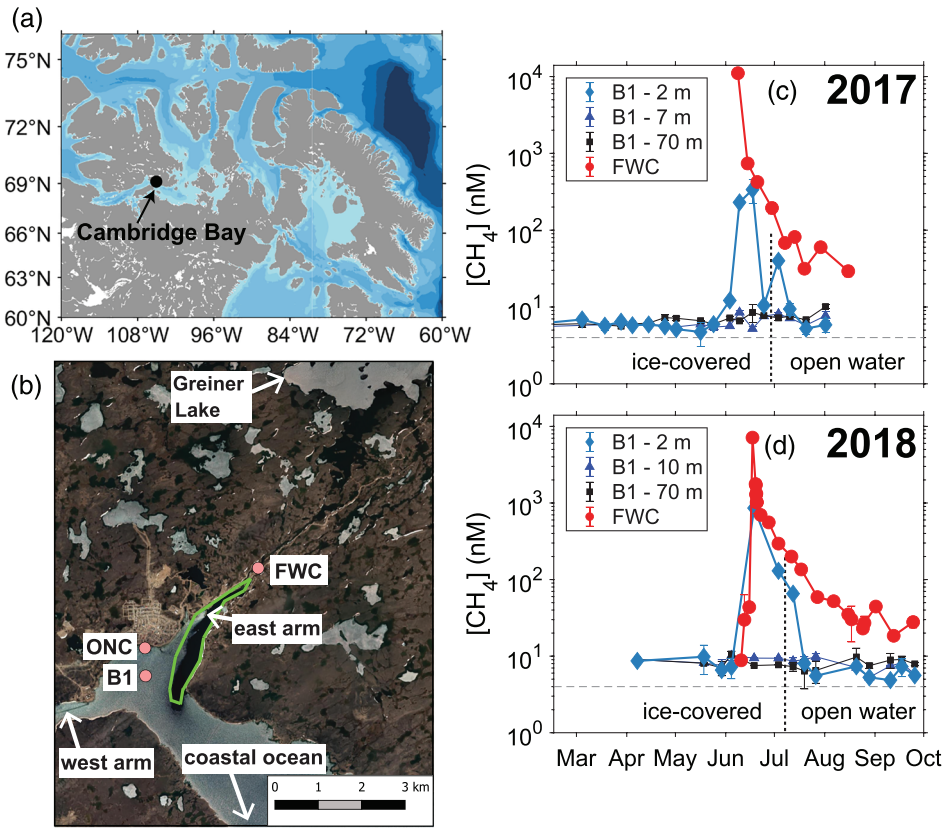

Figure 1. Map of study site and time-series data. (a) Map of eastern Canadian Arctic showing the location of Cambridge Bay. (b) Satellite image of study area on 21 June 2017 (obtained by Google, DigitalGlobe). Pink circles indicate the locations of the main sampling stations FWC (Freshwater Creek) and B1, as well as ONC (ocean networks Canada observatory with ice profiler). The approximate region where the ChemYak was deployed is shown with a green outline. Time-series of CH_4 concentrations in Cambridge Bay estuary and Freshwater Creek in (c) 2017 and (d) 2018. Surface samples in Cambridge Bay were collected at 2 m depth below the ice surface, or 0.75 m below the open water surface. The dashed horizontal line represents atmospheric equilibrium and the dashed vertical line indicates when sampling station B1 became ice-free. Error bars reflect the standard deviation of duplicate measurements.

Ice acts as a barrier to gas exchange, sustaining strong disequilibria in gas concentrations between the atmosphere and ice-covered waters (Butterworth & Miller, 2016; Denfeld et al., 2018; Karlsson et al., 2013; Wand et al., 2006). Rapid reequilibration of the mixed layer can occur following ice melt. Quantifying the impacts of sea ice loss on Arctic greenhouse gas emissions requires seasonally resolved measurements; yet, few measurements of dissolved CH_4 or other greenhouse gases are available in ice-covered or recently ice-liberated Arctic Ocean waters and connected estuaries. Here, we present new observations that address this critical observational gap, demonstrating that the vast majority of annual CH_4 release in an Arctic estuary occurs during the ice melt period.

2. Observations, Results, and Discussion

2.1. Field Observations

To quantify the annual sea-air emissions of greenhouse gases in a coastal Arctic system, we collected measurements in a well-sheltered bay with two inlets (west arm and east arm, Figure 1a) adjacent to the town of Cambridge Bay (Iqaluktuuttiaq), Nunavut, Canada. Surface waters are seasonally ice covered, and the dominant freshwater source is Freshwater Creek, which discharges water into the east arm of Cambridge Bay from Greiner Lake and the associated watershed (mean annual discharge of 1.4×10^8 m^3 $year^{-1}$ from 1970 to 2017). Terrestrial snowmelt in this region typically begins in late May (Tedesco et al., 2009), and, as a result, Freshwater Creek begins to flow before significant sea ice melt has occurred. This freshwater

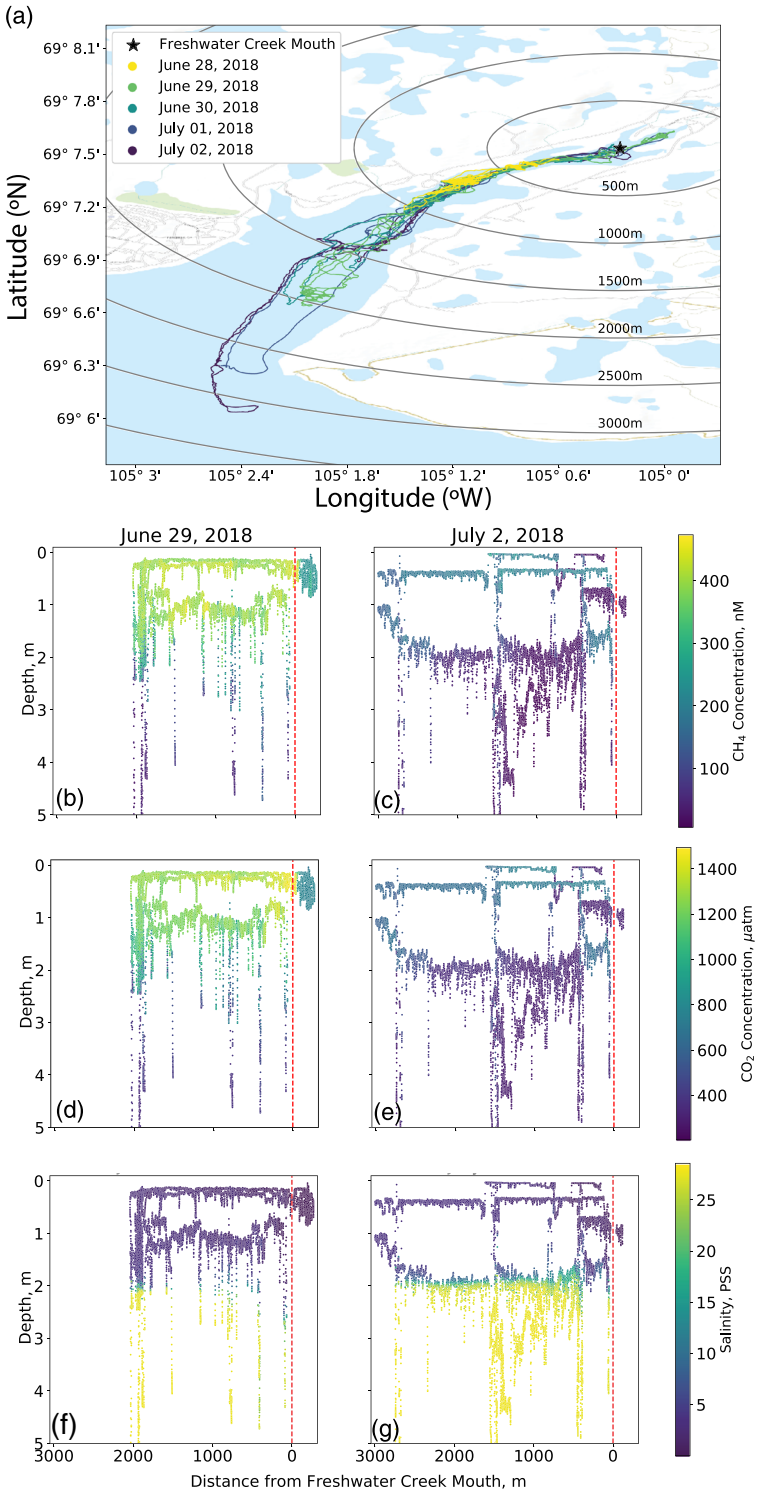

Figure 2. Spatial observations made by the ChemYak vehicle. (a) The study site with ChemYak trajectories from each day overlaid. The mouth of Freshwater Creek (69.1257°N, 105.0042°W) is marked with a star, and concentric rings at increments of 500 m centered at the mouth are provided for scale. Northeast of the red dashed line lies Freshwater Creek (red arrow and box) and a small embayment (blue label and box) which receives input from a much smaller river. (b–g) Observations made by the ChemYak for two representative days, 29 June and 2 July, are plotted by depth versus distance from the Freshwater Creek mouth. Negative distances (to the right of the axis) represent points northeast of the mouth (a small embayment), and positive distance (to the left of the axis) represent points southwest of the mouth (downstream). As indicated by the salinity plots (f, g), the mixed layer depth is <2 m throughout the study area, and the fresh surface layer was generally higher in both CH_4 and CO_2 concentration than layers deeper than 2 m. The gas concentrations decreased over the multiday measurement campaign. Equivalent plots and temperature data for the other measurement days are shown in Figure S5.

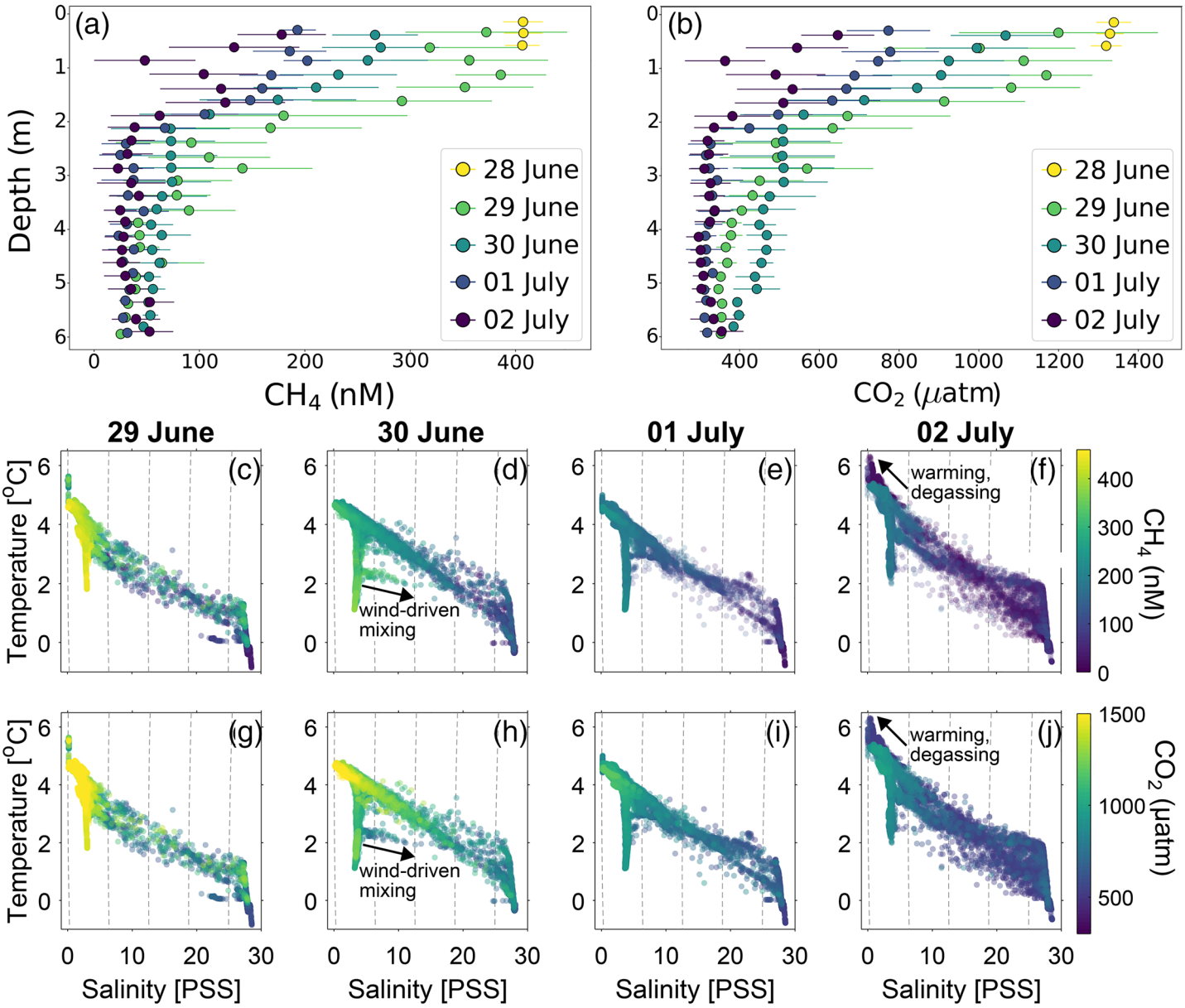

Figure 3. Spatial and temporal trends observed by the ChemYak. (a, b) Each day of the measurement campaign is marked with a unique color, and samples collected are binned into 0.25 m increments from the surface to 6 m. Both CH_4 (a) and CO_2 (b) exhibit decreasing trends for each subsequent day, and there is strong stratification between the surface layer and water below 2 m. Error bars represent the standard deviation of measurements for each depth bin. (c–j) Temperature-salinity plots showing changes in CH_4 (c–f) and CO_2 (g–j) concentrations and water mass distributions over the time-series.

discharge causes the rapid melt of sea ice along the east arm, creating open water in June (Figure 1b), with the rest of the bay typically becoming ice-free 2–3 weeks later, in late June to early July. During 2017 and 2018, we collected a time-series of dissolved CH_4 and N_2O measurements in the estuary and river (Figures 1 and S1 in the supporting information). Additionally, in 2018, we used a remotely operated robotic kayak, the ChemYak (Kimball et al., 2014; Nicholson et al., 2018), to characterize fine-scale spatiotemporal changes in dissolved CH_4 and CO_2 in the estuary during peak river inflow (Figures 2 and 3) and collected water samples from Greiner Lake. Methodological details for bottle samples and the ChemYak are provided in the Supporting Information. The datasets collected by the authors have been archived with PANGAEA (Manning et al., 2019).

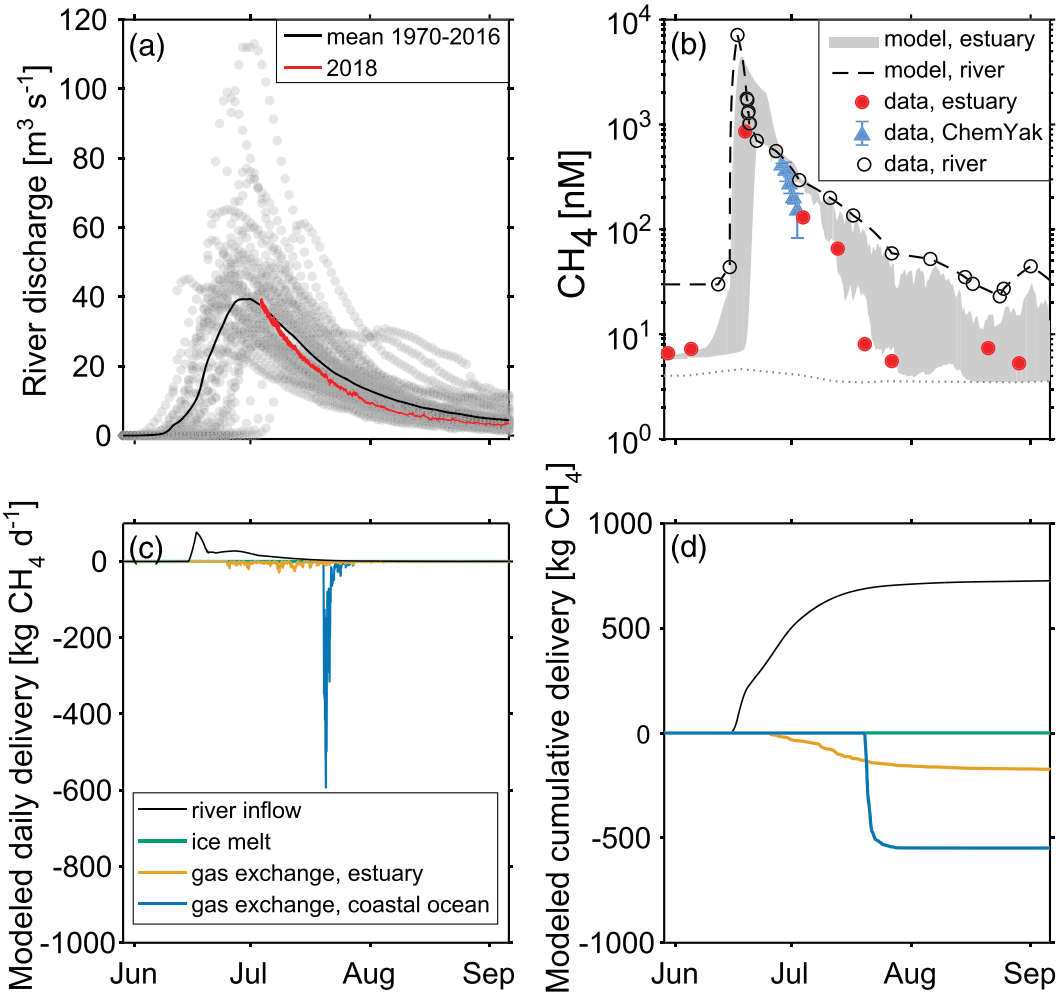

Figure 4. Observations and model-derived output of CH_4 delivery to the estuary mixed layer. (a) historical river discharge data from Freshwater Creek. (b) Modeled and measured CH_4 concentration in the river (Freshwater Creek) and the Cambridge Bay estuary mixed layer (model regions 1 and 2), based on data and the model. The range of modeled values across the estuary is shown with gray shading and the range of values measured with the ChemYak is shown with blue symbols (error bars represent the standard deviation of daily measurements). The red symbols represent bottle measurements at station B1, and the black outlined symbols represent measurements at Freshwater Creek. The gray dotted line shows the equilibrium concentration in the estuary. (c, d) Modeled daily (c) and cumulative (d) CH_4 delivery to the estuary, from river inflow, ice melt, and gas exchange (positive delivery represents an input to the mixed layer). The CH_4 delivery caused by ice melt is negligible relative to the other terms.

During winter and spring (January–May) in 2017 and 2018, CH_4 concentrations throughout the estuary water column (station B1 in Figure 1b) were closely distributed around the atmospheric equilibrium of 4 nM (range 3–10 nM). In early June, river discharge from the spring thaw began to enter the estuary, and elevated CH_4 concentrations up to 860 nM (19,000% saturation) were measured in near-surface waters of Cambridge Bay (2 m below the surface of the ice). A water mass analysis using salinity and water isotope data from station B1 confirmed that the elevated CH_4 concentrations were associated with river runoff rather than ice melt (Figure S2 and Text S1). Ice-free summer surface waters sampled in July 2017 and 2018 had much lower CH_4 concentrations, ranging from 4–65 nM.

In contrast to CH_4, N_2O concentrations throughout 2017 and 2018 at station B1 and Freshwater Creek displayed limited seasonal variability and were close to equilibrium (Figure S1 and Text S2).

From 28 June to 2 July 2018, we used the ChemYak for high-resolution spatial mapping and vertical profiling of CH_4, CO_2, salinity, and temperature distributions in an ~1 km^2 open water area between

the river mouth and the ice edge during the dynamic melt period (Figures 2, 3, and S3–S6). These ChemYak measurements confirmed elevated greenhouse gas concentrations in river-derived estuary water. The river-derived water occurred throughout the study area as a shallow, fresh surface mixed layer (<2 m depth), separated from deeper waters by a sharp pycnocline (Figures 2f and 2g). During the ChemYak measurement period, CH_4 concentrations in the surface water decreased each day and as the water flowed from the river toward the coastal ocean, suggesting a rapid ventilation within the estuary. For example, the CH_4 concentration in Freshwater Creek decreased from 560 ± 10 nM on 27 June to 290 ± 20 nM by 3 July, whereas CH_4 at station B1 was 130 ± 10 nM on 3 July (Figure 4b). In the ChemYak sampling area (between Freshwater Creek and station B1), on 28 June, CH_4 and CO_2 concentrations in the upper 1 m of the water column were up to 470 nM and 1,470 μatm, respectively (mean 410 ± 20 nM and 1340 ± 40 μatm). Concentrations in the upper 1 m decreased over the campaign to 150 ± 70 nM CH_4 and 600 ± 150 μatm CO_2 by 2 July (Figures 3 and S6).

In the estuary, at depths below the mixed layer (>2 m depth), CH_4 and CO_2 concentrations decreased from 29 June to 2 July. Elevated wind speeds (up to 10 m s^{-1}) appear to have enhanced mixing across the sharp pycnocline on 30 June (Figures 3d, 3h, S5, and S6). On 30 June, the depth of the pycnocline shoaled and CH_4 and CO_2 concentrations below the mixed layer increased near the ice edge and the river mouth. Over the following days, lower wind speeds (3.7 ± 1.1 m s^{-1}), coupled with decreasing river inflow concentrations and restratification of the water column, led to decreased gas concentrations throughout the water column by 2 July. Changes in the observed temperature-salinity properties of the water suggest that mixing reduced the vertical salinity gradient over the measurement period. The mixed layer near the river mouth showed significant warming between 28 June and 2 July (Figures 3c–3j, S5, and S6).

To evaluate the importance of atmospheric ventilation to the CH_4 budget in the estuary, we performed sea-air flux calculations (Wanninkhof, 2014) using observed wind speeds. In the absence of lateral transport and river discharge, CH_4 concentrations in the estuary over our sampling period would be expected to decrease to ~70 nM. In actuality, we observed a mean surface CH_4 concentration of ~150 nM at the end of the sampling period, suggesting that the continued inflow of high-CH_4 river water into the ChemYak sampling region contributed to maintaining elevated CH_4 concentrations following ice melt (Figure 4a). Based on the observed river discharge of ~40 m^3 s^{-1}, we estimate that the residence time of water in the ChemYak measurement region was ~0.6 days.

In addition to measuring the estuary downstream of the Freshwater Creek mouth, the ChemYak was also used to collect observations in a small embayment at the outlet of a much smaller river on 29 June, 1 July, and 2 July (Figures 2, 3, S4, and S5). We present the results from this embayment to highlight the complexities of quantifying greenhouse gas fluxes from estuarine systems. This embayment generally exhibited higher temperatures and lower CH_4 and CO_2 concentrations relative to adjacent waters. For example, on 29 June, the mean CH_4 concentration in the upper 2 m was 242 ± 41 nM in the embayment (upstream of the Freshwater Creek mouth), in contrast to 417 ± 31 nM within 100 m downstream of the Freshwater Creek mouth (Figure 2b). For CO_2, the mean concentration was 790 ± 140 μatm in the embayment and 1,400 ± 110 μatm downstream of the Freshwater Creek mouth. In late June to early July 2018, we collected bottle samples at the head of the embayment in this smaller river and found that CH_4 concentrations in Freshwater Creek were two times higher than in the smaller river. The CH_4 and CO_2 levels in the embayment may therefore reflect lower inflowing CH_4 and CO_2 from the smaller river and/or a longer residence time for river-derived surface water to exchange with the atmosphere in the embayment. The observed differences between the smaller river and embayment compared to Freshwater Creek and the rest of the estuary demonstrate the need to conduct studies in a diverse range of Arctic coastal systems to better understand the complex hydrological controls on the magnitude and location of greenhouse gas emissions.

Overall, we conclude that the declining CH_4 and CO_2 concentrations throughout the water column between 28 June and 2 July, and along the spatial gradient from Freshwater Creek to station B1, primarily reflect a combination of decreasing gas concentrations in the river water (Figure 1c), loss due to gas exchange within the ice-liberated area and oceanward lateral advective export. Below, we present a physical model for the estuarine mixed layer CH_4 budget and discuss potential impacts of microbial processes on the CH_4 budget.

2.2. Mixed Layer Model

To quantify the fate of river-derived CH_4 over the entire river inflow season, we developed a mixed layer model for the Cambridge Bay estuary (Figures 4 and S7). The model was constrained with measured CH_4 concentrations in Freshwater Creek (bottle samples), river discharge and wind speed measurements, and ice thickness records from the Ocean Networks Canada (ONC) cabled observatory. The model is described in detail in Figure S7 and Text S3, and the model code, including all input data, is available on GitHub (Manning & Preston, 2020). The results of this analysis suggest that the annual CH_4 cycle in the estuary is driven by river inflow, with sea ice melt contributing a comparatively negligible amount of CH_4 to the mixed layer (Figure 4d). This conclusion is consistent with a water mass property (salinity/water isotope) analysis showing an insignificant impact of sea ice melt on the CH_4 budget (Figure S2 and Text S1).

Using the model, we estimate that ~730 kg CH_4 was released from Freshwater Creek into the estuary in 2018 (volume-weighted mean concentration in river water of 360 nM), with 24% (177 kg) ventilated to the atmosphere from the estuary following ice cover retreat (Figure 4d). The remaining 76% of the river-derived CH_4 was laterally transported across the estuary beneath sea ice to the coastal ocean, where it was likely ventilated to the atmosphere following ice melt in mid-late July. Indeed, a model run with a larger spatial footprint (including 60 km^2 of coastal ocean surrounding the 5 km^2 Cambridge Bay estuary) yielded a cumulative annual sea-air emission of 548 kg CH_4 from the coastal ocean derived from river discharge, which occurs rapidly following ice melt (Figure 4d). To estimate the CH_4 emissions from the estuary in the absence of river inflow, we prescribe a fixed CH_4 concentration of 6 nM (~150% saturation), the typical surface concentration before and after the river inflow period. Under this scenario, with no river discharge, we derived annual estuarine CH_4 emissions of 7.4 kg, 24 times lower than the emissions derived from the full model including riverine CH_4 inputs. Given that our model predicts that 76% of the riverine CH_4 is ventilated beyond the estuary in the adjacent coastal ocean, small river systems such as Freshwater Creek may be of primary importance to annual CH_4 budgets through much of the coastal Arctic Ocean. Accurate calculation of such short-lived, high magnitude CH_4 emissions following ice melt, requires a more extensive under-ice sampling program, including melt-season measurements in multiple river-influenced Arctic estuaries and coastal systems.

The extent of microbial CH_4 oxidation in river-derived water discharged from Freshwater Creek is currently unknown. The early-season river discharge containing >1,000 nM CH_4 may remain under the ice for ~1 month before being exposed to the atmosphere, during which time microbial oxidation could potentially decrease CH_4 levels. Recent incubation studies measuring CH_4 oxidation rates and rate constants in Arctic waters and ice-covered lakes have reported a wide range of values (Bastviken et al., 2002; Bussmann et al., 2017; Gentz et al., 2014; Mau et al., 2013; Rićão Canelhas et al., 2016; Uhlig & Loose, 2017). For example, in an Arctic fjord, Mau et al. (2013) reported first-order CH_4 oxidation rate constants ranging over three orders of magnitude, from ~0.0001 to 0.1 day^{-1}. To determine the maximum possible impact of CH_4 oxidation on the CH_4 budget, we tested a model run incorporating CH_4 oxidation with a rate constant of 0.1 day^{-1} (Text S3 and Figure S9). With this high rate of CH_4 oxidation, the modeled annual CH_4 emissions within the estuary decreased only slightly (from 177 to 164 kg), but CH_4 emissions from the adjacent coastal ocean decreased significantly (from 540 to 130 kg). An oxidation rate of 0.01 day^{-1} yielded emissions of 175 and 480 kg for the estuary and coastal ocean respectively (Figure S9). Overall, these results suggest that microbial oxidation could potentially contribute to a significant reduction in the fraction of laterally exported CH_4 that ultimately is emitted to the atmosphere, but likely has a small impact on CH_4 emissions within the Cambridge Bay estuary. In the future, we hope to measure CH_4 concentration in the coastal ocean adjacent to Cambridge Bay estuary, and CH_4 oxidation rates in Cambridge Bay and adjacent waters, and use these data to improve the model.

3. Conclusions and Future Work

Our results, derived from a year-round times series of CH_4 measurements and dense spatio-temporal observations from a remotely operated robotic kayak, show that CH_4 discharge via Freshwater Creek drives intense CH_4 emissions immediately following ice melt in the Cambridge Bay estuary and surrounding waters. River discharge also acts as a significant seasonal source of CO_2 to the estuary. This study

demonstrates the importance of fully resolving seasonal processes in interconnected marine and freshwater Arctic environments to accurately quantify greenhouse gas emissions. We have also demonstrated the advantages of using new sensing technologies to study heterogeneous and dynamic systems. Similar seasonal variability in CH_4 emissions likely occurs in some other river-influenced, seasonally ice-covered Arctic estuaries, which receive ~10% of global river discharge (Dai & Trenberth, 2002). More field studies in a wide range of Arctic river and coastal systems are needed to determine the impact of ongoing and projected future increases in Arctic river discharge (Macdonald et al., 2015) on greenhouse gas emissions. For example, more extensive measurements of CH_4 concentration and isotopic composition across the land-ocean continuum would assist in determining CH_4 and CO_2 sources and sinks. Radiocarbon measurements would demonstrate whether ancient CH_4 sources such as thawing permafrost are significant (Sparrow et al., 2018). Such studies will provide critical information to characterize current and future Arctic greenhouse gas cycling, improving quantitative estimates of changes in CH_4 and CO_2 emissions.

The low and stable CH_4 concentrations observed below the mixed layer in the Cambridge Bay estuary indicate that sedimentary CH_4 sources within this estuary are negligible relative to river-derived inputs, in contrast to published studies in some other Arctic coastal and shelf systems where significant sedimentary sources are observed (Gentz et al., 2014; Shakhova et al., 2010). Therefore, more research is needed in a wide range of Arctic coastal waters to more accurately characterize the relative importance of terrestrial sources versus subseafloor deposits.

Freshwater input to the Canadian Arctic Archipelago is dominated by small river systems such Freshwater Creek with a collective discharge on the same order as large rivers such as the Mackenzie (Alkire et al., 2017), yet these small rivers are rarely sampled due to challenging conditions. The CH_4 concentrations we measured in Freshwater Creek (ranging from 10–11,000 nM, volume-weighted mean 360 nM) are similar to other river systems in the Arctic and worldwide. For example, mean CH_4 concentrations observed in the Yukon River, Lena Delta, and Leverett Glacier runoff range from 70–750 nM (Bussmann, 2013; Lamarche-Gagnon et al., 2019; Striegl et al., 2012). Furthermore, a data compilation of over 900 rivers and streams worldwide reported a mean CH_4 concentration of 1,400 $\pm$ 5,200 nM and median of 250 nM (Stanley et al., 2016). The peak CH_4 concentrations observed in Cambridge Bay estuary (up to 900 nM during the freshet, prior to ice melt) are similar to maximum values measured in other Arctic coastal waters (Bussmann et al., 2017; Shakhova et al., 2010).

The results of this study motivate future coastal Arctic field campaigns at other sites with measurement technologies capable of high spatial and temporal resolution mapping immediately before and during ice melt. Such studies will provide critical information to characterize current and future Arctic greenhouse gas emission, improving quantitative estimates of changes in CH_4 and CO_2 emissions across the rapidly changing Arctic environment.

Acknowledgments
All data generated by the authors that were used in this article are available on PANGAEA (https://doi.org/10.1594/PANGAEA.907159) and model code for estimating CH_4 transport is available on GitHub (https://doi.org/10.5281/zenodo.3785893). We acknowledge the use of imagery from the NASA Worldview application (https://worldview.earthdata.nasa.gov), part of the NASA Earth Observing System Data and Information System (EOSDIS), and data from Ocean Networks Canada, and Environment Canada. We thank everyone involved in the fieldwork including C. Amegainik, Y. Bernard, A. Cranch, F. Emingak, S. Marriott, and A. Pedersen. Laboratory analysis and experiments were performed by A. Cranch, R. McCulloch, A. Morrison, and Z. Zheng. We thank J. Brinckerhoff, the Arctic Research Foundation, and the staff of the Canadian High Arctic Research Station for support with field logistics. Funding for the work was provided by MEOPAR NCE funding to B. Else, a WHOI Interdisciplinary Award to A. Michel., D. Nicholson. and S. Wankel, and Canadian NSERC grants to P. Tortell. and B. Else. Authors received fellowships, scholarships, and travel grants including an NSERC postdoctoral fellowship to C. Manning, an NDSEG fellowship to V. Preston, NSERC PGS-D and Izaak Walton Killam Pre-Doctoral scholarships to S. Jones, and Northern Scientific Training Program funds (Polar Knowledge Canada, administered by the Arctic Institute of North America, University of Calgary) to S. Jones and P. Duke. We also thank Polar Knowledge Canada (POLAR) and Nunavut Arctic College for laboratory space and field logistics support.

References

Alkire, M. B., Jacobson, A. D., Lehn, G. O., Macdonald, R. W., & Rossi, M. W. (2017). On the geochemical heterogeneity of rivers draining into the straits and channels of the Canadian Arctic archipelago. *Journal of Geophysical Research: Biogeosciences*, *122*(10), 2527–2547. https://doi.org/10.1002/2016JG003723

Bastviken, D., Ejlertsson, J., & Tranvik, L. (2002). Measurement of methane oxidation in lakes: A comparison of methods. *Environmental Science & Technology*, *36*(15), 3354–3361. https://doi.org/10.1021/es010311p

Biastoch, A., Treude, T., Rüpke, L. H., Riebesell, U., Roth, C., Burwicz, E. B., et al. (2011). Rising Arctic Ocean temperatures cause gas hydrate destabilization and ocean acidification. *Geophysical Research Letters*, *38*(8), L08602. https://doi.org/10.1029/2011GL047222

Bussmann, I. (2013). Distribution of methane in the Lena Delta and Buor-Khaya bay, Russia. *Biogeosciences*, *10* (7), 4641–4652. https://doi.org/10.5194/bg-10-4641-2013

Bussmann, I., Hackbusch, S., Schaal, P., & Wichels, A. (2017). Methane distribution and oxidation around the Lena Delta in summer 2013. *Biogeosciences*, *14*(21), 4985–5002. https://doi.org/10.5194/bg-14-4985-2017

Butterworth, B. J., & Miller, S. D. (2016). Air-sea exchange of carbon dioxide in the Southern Ocean and Antarctic marginal ice zone. *Geophysical Research Letters*, *43*(13), 7223–7230. https://doi.org/10.1002/2016GL069581

Dai, A., & Trenberth, K. E. (2002). Estimates of freshwater discharge from continents: Latitudinal and seasonal variations. *Journal of Hydrometeorology*, *3*(6), 660–687. https://doi.org/10.1175/1525-7541(2002)003<0660:EOFDFC>2.0.CO;2

Denfeld, B. A., Baulch, H. M., Giorgio, P. A. del, Hampton, S. E., & Karlsson, J. (2018). A synthesis of carbon dioxide and methane dynamics during the ice-covered period of northern lakes. *Limnology and Oceanography Letters*, *3*(3), 117–131. https://doi.org/10.1002/lol2.10079

Fenwick, L., Capelle, D., Damm, E., Zimmermann, S., Williams, W. J., Vagle, S., & Tortell, P. D. (2017). Methane and Nitrous Oxide Distributions across the North American Arctic Ocean during Summer, 2015. *Journal of Geophysical Research: Oceans, 122*, 1–23. https://doi.org/10.1002/2016JC012493

Gentz, T., Damm, E., Schneider von Deimling, J., Mau, S., McGinnis, D. F., & Schlüter, M. (2014). A water column study of methane around gas flares located at the West Spitsbergen continental margin. *Continental Shelf Research*, *72*, 107–118. https://doi.org/10.1016/j.csr.2013.07.013

James, R. H., Bousquet, P., Bussmann, I., Haeckel, M., Kipfer, R., Leifer, I., et al. (2016). Effects of climate change on methane emissions from seafloor sediments in the Arctic Ocean: A review. *Limnology and Oceanography*, *61*(S1), S283–S299. https://doi.org/10.1002/lno.10307

Karlsson, J., Giesler, R., Persson, J., & Lundin, E. (2013). High emission of carbon dioxide and methane during ice thaw in high latitude lakes. *Geophysical Research Letters*, *40* (6), 1123–1127. https://doi.org/10.1002/grl.50152

Kimball, P., Bailey, J., Das, S., Geyer, R., Harrison, T., Kunz, C., et al. (2014). The WHOI Jetyak: An autonomous surface vehicle for oceanographic research in shallow or dangerous waters. *2014 IEEE/OES Autonomous Underwater Vehicles (AUV)*, *1*, 7. https://doi.org/10.1109/AUV.2014.7054430

Kvenvolden, K. A., Lilley, M. D., Lorenson, T. D., Barnes, P. W., & McLaughlin, E. (1993). The Beaufort Sea continental shelf as a seasonal source of atmospheric methane. *Geophysical Research Letters*, *20*(22), 2459–2462. https://doi.org/10.1029/93GL02727

Lamarche-Gagnon, G., Wadham, J. L., Sherwood Lollar, B., Arndt, S., Fietzek, P., Beaton, A. D., et al. (2019). Greenland melt drives continuous export of methane from the ice-sheet bed. *Nature*, *565*(7737), 73–77. https://doi.org/10.1038/s41586-018-0800-0

Macdonald, R. W., Kuzyk, Z. A., & Johannessen, S. C. (2015). It is not just about the ice: A geochemical perspective on the changing Arctic Ocean. *Journal of Environmental Studies and Sciences*, *5*(3), 288–301. https://doi.org/10.1007/s13412-015-0302-4

Magnuson, J. J. (2000). Historical trends in Lake and river ice cover in the northern hemisphere. *Science*, *289*(5485), 1743–1746. https://doi.org/10.1126/science.289.5485.1743

Manning, C. C., & Preston, V. L. (2020). Caramanning/Cambridge-bay-model: Cambridge Bay model with optional methane oxidation term (version 1.3). *Zenodo*. https://doi.org/10.5281/zenodo.3785893

Manning, C. C., Preston, V. L., Jones, S. F., Michel, A. P. M., Nicholson, D. P., Duke, P. J., et al. (2019): Dissolved methane, nitrous oxide, carbon dioxide, water isotope, salinity and temperature data from Cambridge Bay, Nunavut, Canada (2017-2018). *PANGAEA*, https://doi.org/10.1594/PANGAEA.907159

Mau, S., Blees, J., Helmke, E., Niemann, H., & Damm, E. (2013). Vertical distribution of methane oxidation and methanotrophic response to elevated methane concentrations in stratified waters of the Arctic fjord Storfjorden (Svalbard, Norway). *Biogeosciences*, *10*, 6267–6278. https://doi.org/10.5194/bg-10-6267-2013

Nicholson, D. P., Michel, A. P. M., Wankel, S. D., Manganini, K., Sugrue, R. A., Sandwith, Z. O., & Monk, S. A. (2018). Rapid mapping of dissolved methane and carbon dioxide in coastal ecosystems using the ChemYak autonomous surface vehicle. *Environmental Science & Technology*, *52*(22), 13,314–13,324. https://doi.org/10.1021/acs.est.8b04190

Phelps, A. R., Peterson, K. M., & Jeffries, M. O. (1998). Methane efflux from high-latitude lakes during spring ice melt. *Journal of Geophysical Research: Atmospheres*, *103*(D22), 29,029–29,036. https://doi.org/10.1029/98JD00044

Ricão Canelhas, M., Denfeld, B. A., Weyhenmeyer, G. A., Bastviken, D., & Bertilsson, S. (2016). Methane oxidation at the water-ice interface of an ice-covered lake. *Limnology and Oceanography*, *61*(S1), S78–S90. https://doi.org/10.1002/lno.10288

Shakhova, N., Semiletov, I., Salyuk, A., Yusupov, V., Kosmach, D., & Gustafsson, Ö. (2010). Extensive methane venting to the atmosphere from sediments of the east Siberian Arctic shelf. *Science*, *327*(5970), 1246–1250. https://doi.org/10.1126/science.1182221

Sparrow, K. J., Kessler, J. D., Southon, J. R., Garcia-Tigreros, F., Schreiner, K. M., Ruppel, C. D., et al. (2018). Limited contribution of ancient methane to surface waters of the U.S. Beaufort Sea shelf. *Science Advances* (1), eaao4842. https://doi.org/10.1126/sciadv.aao4842

Stanley, E. H., Casson, N. J., Christel, S. T., Crawford, J. T., Loken, L. C., & Oliver, S. K. (2016). The ecology of methane in streams and rivers: Patterns, controls, and global significance. *Ecological Monographs*, *86*(2), 146–171. https://doi.org/10.1890/15-1027.1

Striegl, R. G., Dornblaser, M. M., McDonald, C. P., Rover, J. R., & Stets, E. G. (2012). Carbon dioxide and methane emissions from the Yukon River system. *Global Biogeochemical Cycles*, *26*(4). https://doi.org/10.1029/2012GB004306

Stroeve, J. C., Serreze, M. C., Holland, M. M., Kay, J. E., Malanik, J., & Barrett, A. P. (2012). The Arctic's rapidly shrinking sea ice cover: A research synthesis. *Climatic Change*, *110*(3–4), 1005–1027. https://doi.org/10.1007/s10584-011-0101-1

Tedesco, M., Brodzik, M., Armstrong, R., Savoie, M., & Ramage, J. (2009). Pan Arctic terrestrial snowmelt trends (1979–2008) from spaceborne passive microwave data and correlation with the Arctic oscillation. *Geophysical Research Letters*, *36*(21). https://doi.org/10.1029/2009GL039672

Uhlig, C., & Loose, B. (2017). Using stable isotopes and gas concentrations for independent constraints on microbial methane oxidation at Arctic Ocean temperatures. *Limnology and Oceanography: Methods*, *15*(8), 737–751. https://doi.org/10.1002/lom3.10199

Voigt, C., Marushchak, M. E., Lamprecht, R. E., Jackowicz-Korczyński, M., Lindgren, A., Mastepanov, M., et al.. (2017). Increased nitrous oxide emissions from Arctic peatlands after permafrost thaw. *Proceedings of the National Academy of Sciences*, *114*(24), 6238–6243. https://doi.org/10.1073/pnas.1702902114

Wand, U., Samarkin, V. A., Nitzsche, H.-M., & Hubberten, H.-W. (2006). Biogeochemistry of methane in the permanently ice-covered Lake Untersee, central Dronning Maud land, East Antarctica. *Limnology and Oceanography*, *51*(2), 1180–1194. https://doi.org/10.4319/lo.2006.51.2.1180

Wanninkhof, R. (2014). Relationship between wind speed and gas exchange over the ocean revisited. *Limnology and Oceanography: Methods*, *12*(6), 351–362. https://doi.org/10.4319/lom.2014.12.351

Zona, D., Gioli, B., Commane, R., Lindaas, J., Wofsy, S. C., Miller, C. E., et al. (2016). Cold season emissions dominate the Arctic tundra methane budget. *Proceedings of the National Academy of Sciences of the United States of America*, *113*(1), 40–45. https://doi.org/10.1073/pnas.1516017113

References From the Supporting Information

Anderson, L. G., Turner, D. R., Wedborg, M., & Dyrssen, D. (1999). Determination of Total Alkalinity and Total Dissolved Inorganic Carbon. In K. Grasshoff,K. Kremling, & M. Ehrhardt, (Eds.), *Methods of Seawater Analysis* (pp. 127–148).

Naqvi, S. W. A., Bange, H. W., Farías, L., Monteiro, P. M. S., Scranton, M. I., & Zhang, J. (2010). Marine hypoxia/anoxia as a source of CH_4 and N_2O. *Biogeosciences*,*7*(7), 2159–2190. https://doi.org/10.5194/bg-7-2159-2010

Bliss, L. C. (1981). North American and Scandinavian tundras and polar deserts. In L. C. Bliss, O. W. Heal, & J. J. Moore (Eds.), *Tundra ecosystems: A comparative analysis* (pp. 8–14). Cambridge, UK: Cambridge University Press.

Cai, W.-J., Hu, X., Huang, W.-J., Jiang, L.-Q., Wang, Y., Peng, T.-H., & Zhang, X. (2010). Alkalinity distribution in the western North Atlantic Ocean margins. *Journal of Geophysical Research: Oceans*, *115*(C8). https://doi.org/10.1029/2009JC005482

Capelle, D. W., Dacey, J. W., & Tortell, P. D. (2015). An automated, high through-put method for accurate and precise measurements of dissolved nitrous-oxide and methane concentrations in natural waters: Automated PT-GCMS for N_2O and CH_4. *Limnology and Oceanography: Methods*, *13*(7), 345–355. https://doi.org/10.1002/lom3.10029

Dickson, A. G. (1990). Thermodynamics of the dissociation of boric acid in synthetic seawater from 273.15 to 318.15 K. *Deep Sea Research Part A. Oceanographic Research Papers*, *37*(5), 755–766. https://doi.org/10.1016/0198-0149(90)90004-F

Environment and Climate Change Canada Historical Database (2019) Hourly weather data for Cambridge Bay, Nunavut from Jan 1, 2018 to Jan 1, 2019. Station Climate ID: 2400602, WMO ID: 71288 TC ID: XCM http://climate.weather.gc.ca . Downloaded on February 25, 2019.

Environment and Climate Change Canada Historical Hydrometric Data website, River discharge data for station 10TF001, Freshwater Creek near Cambridge Bay https://wateroffice.ec.gc.ca/mainmenu/historical_data_index_e.html. Water Survey of Canada, Environment and Climate Change Canada. Downloaded on January 10, 2019.

Lee, K., Kim, T.-W., Byrne, R. H., Millero, F. J., Feely, R. A., & Liu, Y.-M. (2010). The universal ratio of boron to chlorinity for the North Pacific and North Atlantic oceans. *Geochimica et Cosmochimica Acta*, *74*(6), 1801–1811. https://doi.org/10.1016/j.gca.2009.12.027

Macdonald, R. W., Paton, D. W., Carmack, E. C., & Omstedt, A. (1995). The freshwater budget and under-ice spreading of Mackenzie River water in the Canadian Beaufort Sea based on salinity and 18O/16O measurements in water and ice. *Journal of Geophysical Research: Oceans*, *100*(C1), 895–919. https://doi.org/10.1029/94JC02700

Millero, F. J. (2010). Carbonate constants for estuarine waters. *Marine and Freshwater Research*, *61*(2), 139–142. https://doi.org/10.1071/MF09254

Ocean Networks Canada Data Archive (2019). Corrected ice draft data from Cambridge Bay, Nunavut, from Jan 1, 2018 to Jan 1, 2019, Sensor ID 21593, Device ID 24049. http://www.oceannetworks.ca, Ocean Networks Canada, University of Victoria, Canada. Downloaded on May 25, 2019.

Pierrot, D., Lewis, E., & Wallace, D. W. R. (2006). *MS Excel Program Developed for CO2 System Calculations* (Technical Report). Oak Ridge, Tenn: Carbon Dioxide Inf. Anal. Cent., Oak Ridge Natl. Lab., US DOE.

Seitzinger, S. P., & Kroeze, C. (1998). *Global Distribution of Nitrous Oxide Production and N Inputs in Freshwater and Coastal Marine Ecosystems*, *12*(1), 93–113.

Seitzinger, S.P., Kroeze, C., & Styles, R.V. (2000). Global distribution of N2O emissions from aquatic systems: Natural emissions and anthropogenic effects. *Chemosphere: Global Change Science*, *2*, 267–279. https://doi.org/10.1016/S1465-9972(00)00015-5

Weiss, R. F., & Price, B. A. (1980). Nitrous oxide solubility in water and seawater. *Marine Chemistry 8*(4), 347–359. https://doi.org/10.1016/0304-4203(80)90024-9

Wiesenburg, D. A., & Guinasso, N. L. (1979). Equilibrium solubilities of methane, carbon monoxide, and hydrogen in water and sea water. *Journal of Chemical & Engineering Data*, *24*(4), 356–360. https://doi.org/10.1021/je60083a006

Wilson, S. T., Bange, H. W., Arévalo-Martínez, D. L., Barnes, J., Borges, A. V., Brown, I., et al. (2018). An intercomparison of oceanic methane and nitrous oxide measurements. *Biogeosciences*, *15*(19), 5891–5907. https://doi.org/10.5194/bg-15-5891-2018

Yamamoto, S., Alcauskas, J. B., & Crozier, T. E. (1976). Solubility of methane in distilled water and seawater. *Journal of Chemical & Engineering Data*, *21*(1), 78–80. https://doi.org/10.1021/je60068a029

Yamamoto-Kawai, M., McLaughlin, F. A., Carmack, E. C., Nishino, S., Shimada, K., & Kurita, N. (2009). Surface freshening of the Canada Basin, 2003-2007: River runoff versus sea ice meltwater. *Journal of Geophysical Research: Oceans*, *114*(4), 2003–2007. https://doi.org/10.1029/2008JC005000

Zhou, J., Delille, B., Eicken, H., Vancoppenolle, M., Brabant, F., Carnat, G., et al. (2013). Physical and biogeochemical properties in landfast sea ice (Barrow, Alaska): Insights on brine and gas dynamics across seasons. *Journal of Geophysical Research: Oceans*, *118*(6), 3172–3189. https://doi.org/10.1002/jgrc.20232